Title

Electrophysiological signatures of acute systemic lipopolysaccharide: potential implications for delirium science

Author List

*Ziyad W Sultan, BS[a]
*Elizabeth R Jaeckel, BS[b]
Bryan M Krause, PhD[a]
Sean M Grady, BS[a]
Caitlin A Murphy, PhD[a]
Robert D Sanders, BSc (Hons) MBBS PhD DABA FRCA[c,d]
Matthew I Banks, PhD[a]

* these authors contributed equally

Affiliations

a – Department of Anesthesiology, School of Medicine and Public Health, University of Wisconsin–Madison
b – Department of Pharmacology, University of Michigan Medical School
c – Specialty of Anaesthetics, Faculty of Medicine and Health, University of Sydney
d – Department of Anaesthetics, Royal Prince Alfred Hospital, Camerpdown, New South Wales, Australia

Corresponding Author

Matthew I Banks, PhD
Professor
Department of Anesthesiology
4605 Medical Sciences Center
1300 University Avenue
Madison, WI 53706
608-261-1143
mibanks@wisc.edu

Abstract

Background: Novel preventive therapies are needed for postoperative delirium, which especially affects aged patients. A mouse model is presented that captures inflammation-associated cortical slow wave activity (SWA) observed in patients, allowing exploration of the mechanistic role of prostaglandin-adenosine signaling.

Methods: EEG and cortical cytokine measurements (interleukin 6 [IL-6], monocyte chemoattractant protein-1 [MCP-1]) were obtained from adult and aged mice. Behavior, SWA, and functional connectivity (alpha-band weighted phase lag index) were assayed before and after systemic administration of lipopolysaccharide (LPS) +/- piroxicam (cyclooxygenase inhibitor) or caffeine (adenosine receptor antagonist). To avoid confounds from inflammation-driven changes in movement, which alter SWA and connectivity, electrophysiological recordings were classified as occurring during quiescence or movement, and propensity score matching used to match distributions of movement magnitude between baseline and LPS.

Results: LPS produces increases in cortical cytokines and behavioral quiescence. In movement-matched data, LPS produces increases in SWA (likelihood-ratio test: $\chi^2(4)=21.51$, $p=0.00057$), but not connectivity ($\chi^2(4)=6.39$, $p=0.17$). Increases in SWA associate with IL6 ($p<0.001$) and MCP-1 ($p=0.001$) and are suppressed by piroxicam ($p<0.001$) and caffeine ($p=0.046$). Aged animals compared to adult show similar LPS-induced SWA during movement, but exaggerated cytokine response and increased SWA during quiescence.

Conclusions: Cytokine-SWA correlations during wakefulness are consistent with observations in patients with delirium. Absence of connectivity effects after accounting

for movement changes suggests decreased connectivity in patients is a biomarker of hypoactivity. Exaggerated effects in quiescent aged animals are consistent with increased hypoactive delirium in older patients. Prostaglandin-adenosine signaling may link inflammation to neural changes and hence delirium.

Keywords

Functional connectivity, delirium, electroencephalography, cytokines, slow wave activity

Introduction

Inflammation is a key mechanism of many neurological disorders, be they chronic, such as dementia, or acute, such as delirium[1–6]. Even in less severe cases, acute inflammation affects brain function through illnesses including the common cold or influenza, causing neurological effects such as somnolence[7]. Elucidation of how inflammation affects brain function could highlight therapeutic targets to reduce the burden of these conditions.

Delirium is an acute disturbance of consciousness characterized by reduced attention, disorganized thinking, and fluctuating arousal levels that often affects sick elderly patients, especially those undergoing high risk surgery[8–12]. The electrophysiological hallmark of delirium is EEG slow wave activity (SWA)[13, 14], similar to that observed during non-rapid eye movement sleep. SWA during delirium seems to particularly involve posterior brain regions[14]. Although evidence suggests that SWA during natural overnight sleep is restorative and enhances cognitive function, SWA during wakefulness, as occurs in delirium, is associated with cognitive deficits[15]. We have suggested that SWA may precipitate cognitive disintegration in delirium, such that patients are awake and confused[1]. Inflammation is the predominant acute cause of delirium[1, 14, 16]; it drives somnolence and enhances SWA in sleep[17–19], and inflammation may similarly drive SWA in delirium[20]. In elderly patients, EEG SWA correlates with delirium severity, plasma cytokines, and EEG connectivity[14]. Our overarching hypothesis is that inflammation drives acute changes in SWA and disrupted cortical connectivity during wakefulness, triggering sudden and profound impairment in

cognition. Herein, we test the link between inflammation and changes in brain activity and connectivity in a mouse model.

Progress on developing therapeutic interventions for delirium has been limited due to the lack of an established animal model to provide insights into its pathogenesis. The most critical limitation has been in identifying translational biomarkers of this complex human cognitive disorder. Recognizing the difficulty in establishing an animal model for these cognitive deficits, we focus on a translational biomarker of delirium, SWA in the EEG, building on previous work[21, 22]. In a critical advance from this earlier work, we focus on (i) SWA specific to active wakefulness, (ii) inflammation as the primary trigger, and (iii) how age may modulate these two factors, consistent with age being a key predisposing factor to delirium. Furthermore, we test interventions that attenuate the behavioral consequences of LPS. Based on prior studies showing that cyclooxygenase inhibitors attenuate acute behavioral changes induced by LPS by inhibiting the prostaglandin response[3, 23], and that prostaglandins act as somnogens via adenosine signaling[24, 25], we investigated the role of prostaglandin – adenosine signaling in linking inflammation to changes in neural activity and connectivity.

Materials and Methods

Further methodological details can be found in Supplementary Methods online.

Data collection

All procedures with animals were approved by the University of Wisconsin-Madison Institutional Animal Care and Use Committee (IACUC) and in full accordance with Research Animal Resources and Compliance (RARC). Adult (2-8 months old; n=68) and aged (16-24 months old, n=14) c57Bl/6J mice were used in this study (Supplementary Table 1). Of these 82 mice, 72 were instrumented for skull screw EEG recordings (bilateral parietal and frontal electrodes). After 5-7 days recovery, animal activity, resting-state EEG, and anterior-posterior functional connectivity were assayed during the animals' dark (active) phase during a 1hr baseline period and for several hours after treatments, after which animals were euthanized and their brains frozen for later cytokine ELISA (Supplementary Figures 1 & 7). For LPS-alone experiments, animals were recorded 1 hour before and for 4 hours after intraperitoneal (IP) LPS administration at t=0hr (vehicle=0.9% NaCl, Low LPS=12.5 or 25µg/kg, High LPS=125µg/kg). For piroxicam experiments, recordings commenced at t=-2hr, piroxicam (10mg/kg IP) was administered at t=-1hr, followed by LPS (25µg/kg) at t=0hr, and euthanasia at t=4hr. Because caffeine has a short half-life in mice (<1hr)[26], three IP injections of caffeine citrate (30mg/kg) were administered: the first at t=0hr (along with LPS 25µg/kg), then at t=1hr and t=2hr. To monitor movement and activity levels, video was recorded for the duration of electrophysiological recording and analyzed offline.

Data analysis

Band power analysis of EEG data proceeded according to standard techniques[27], with power calculated in 4-second sliding windows in the delta (i.e. SWA, 2-4Hz), theta (4-12Hz), alpha (13- 20Hz), beta (20-30Hz), and gamma (30-80Hz) bands and normalized by total power. Functional connectivity was assayed using the alpha band debiased weighted phase lag index (wPLI)[28], calculated in 20-second sliding windows between anterior and posterior channel pairs for each hemisphere, and averaged across hemispheres. We chose alpha band wPLI *a priori* because it is a standard metric of functional connectivity[27] and is used especially in other papers on delirium[14, 29, 30]. A movement signal, derived from the smoothed and normalized frame-by-frame video difference signal, was aligned in time with the simultaneously recorded EEG signal, and the movement signal averaged in each 4-sec or 20-sec epoch for band power and wPLI analysis, respectively. Epochs with nonzero estimated movement were used to calculate electrophysiological parameters corresponding to active wakefulness. To ensure that drug-induced changes in activity level for epochs classified as active wakefulness did not influence measured electrophysiological parameters, distributions of movement signal magnitude were matched between baseline and treatment periods using propensity score matching (PSM; Supplementary Figure 2)[31].

Cytokine quantification was applied to brains from 46 mice with EEG recordings and 10 uninstrumented mice subjected to identical drug treatments (Supplementary Table 1). The cytokines interleukin 6 (IL-6) and monocyte chemoattractant protein-1 (MCP-1) were quantified by multiplex ELISA performed by Eve Technologies (#MDF10, Calgary, AB, Canada). IL-6 was selected *a priori* as the primary cytokine of interest, as

brain levels of IL-6 increase dramatically in the hours following peripheral treatment with LPS[32], with IL-6 having a relatively long half-life compared to other cytokines[33], and IL-6 tends to be higher in hip-fracture surgical patients with delirium compared to those without[34]. Additionally, MCP-1 was chosen based on our recent findings in humans showing that MCP-1 correlates with delirium severity and EEG slow wave activity[14].

To compare LPS-driven changes in EEG and activity measures across time, data were averaged across epochs during a “peak effect” period (t=1 to 3hrs post-injection) and compared to the average across epochs during the “baseline” pre-injection period (t=-1 to 0hr). LPS effects on band power, movement, and wPLI were assessed by fitting linear mixed effects models[35]. Fixed effects were treatment group, experiment epoch (baseline vs. peak effect), and their interaction, with random effects for animal to account for repeated measures and for multiple electrodes within animals when appropriate. Models fit to cytokine data used group and region (anterior/posterior) as fixed effects.

LPS dose categories were as follows: “Vehicle” (n=7) corresponded to 0µg/kg (i.e. 0.9% NaCl alone), “Low LPS” to 12.5µg/kg (n=8) and 25µg/kg (n=15) (grouped together as the outcomes of statistical analyses were unchanged by grouping the low doses), and "High LPS" (n=8) to 125µg/kg. Effects of LPS were tested by comparing models with and without the group-by-epoch interaction (or group-by-region for cytokine data) using likelihood ratio tests. Caffeine and the associated saline controls were fit in separate models from the other groups due to their differing experiment schedule, which may have affected behavior and precluded direct comparisons of these groups to the others. Post-hoc comparisons used the Kenward-Roger method and p-values were

adjusted for the family of relevant multiple comparisons by estimating a multivariate t-distribution using the emmeans package for R[36].

For relationships between cytokine levels and changes in movement-matched SWA, we fit a linear model to all data in the Vehicle, Low LPS, and High LPS groups to estimate SWA as a function of cytokine concentration. We then predicted SWA changes based on cytokine levels observed in the PXM + Low LPS group and tested whether the mean residual differed from zero using a one-sample t-test.

Results

LPS injection increases inflammatory markers in the brain

We first used ELISA to measure protein levels of proinflammatory cytokines IL-6 and MCP-1 (Figure 1A-B) in anterior or posterior mouse neocortex (*purple* and *green,* respectively) four hours after IP injection of LPS. There was no interaction between region and LPS dose for IL-6 (likelihood ratio test adding location: $\chi^2(4)=4.30$, $p=0.37$) or MCP-1 (likelihood ratio test adding location: $\chi^2(4)=6.85$, $p=0.14$); thus, we averaged anterior and posterior samples. IL-6 and MCP-1 levels were elevated following LPS injection, and there was a significant overall effect of LPS group on cytokine concentration (Table 1A-B). Cytokine levels in Vehicle animals were not different from Low LPS animals, though both groups had significantly lower cytokine levels compared to High LPS.

LPS injection increases SWA and decreases antero-posterior connectivity

LPS administration was followed by a slowing of resting-state brain activity, manifest as an increase in SWA in the EEG signal (Figure 2A-B) and a concomitant decrease in amplitude in higher frequency bands, such as gamma (Supplementary Figure 3). SWA band power showed clear changes following LPS injection, with the effect reaching a peak between 1- and 3-hours post-injection ("peak LPS"; Figure 2B). Increases in SWA from baseline to peak LPS significantly depended on LPS dose (Table 1C). Similarly, decreases in gamma power following LPS treatment were dose-dependent (Supplementary Figure 4A; Table 1D). In a regional analysis of SWA we found a significant interaction between anterior/posterior region, group, and time

(likelihood ratio test: $\chi^2(3)=8.82$, p=0.032). However, this effect was limited to a larger posterior compared to anterior increase in the High LPS animals, which could be explained by ceiling effects specifically in the High LPS condition (at baseline, anterior SWA was greater than posterior power in all groups). Since animals in all subsequent experiments received either Vehicle or Low LPS, and because the LPS effect was comparable anterior and posterior in the Low LPS group, we did not alter our *a priori* statistical plan to combine anterior and posterior channels in analyses of power.

Previous reports have suggested that cortical functional connectivity (measured by alpha-band wPLI) is disrupted in delirious patients[14, 29], and systemic LPS can alter connectivity in human volunteers[37]. Consistent with these previous observations, we observed decreased alpha-band wPLI following injection of LPS (Figure 2C). Alpha-band connectivity decreased more in Low LPS and High LPS animals compared to Vehicle, though there was no difference between LPS doses (Table 1E).

LPS decreases movement

Animals injected with LPS exhibited sickness behavior typical of systemic inflammation, including piloerection, hunched posture, and reduced locomotion and grooming activity[38]. The effect of LPS on overall activity level was quantified by the magnitude of the movement signal derived from the video recordings (Supplementary Figure 5, *black*; see Methods). Consistent with prior observations[39], LPS caused a dramatic decrease in movement from baseline to peak LPS hours (Figure 2D). Movement decreased more in Low LPS and High LPS animals compared to Vehicle, though there was no significant difference between LPS doses (Table 1F).

228

229 **SWA in LPS increases after correcting for changes in movement**

230 Because EEG delta power is higher and gamma power is lower during sleep and
231 quiescent wakefulness compared to active wakefulness[40, 41], the changes in movement
232 following LPS injection could themselves account for the observed slowing in EEG
233 signals. In all animals, movement was negatively correlated with SWA (Supplementary
234 Figure 5; Supplementary Figure 6A; $r^{2=}0.313$, $p<0.05$). Because delirium in patients is
235 characterized by elevated delta power during wakefulness[13, 14], we tested whether LPS
236 caused a slowing of the EEG after accounting for the LPS-induced decrease in
237 movement.

238 In an exploratory analysis, we calculated power spectral density in overlapping 4-
239 second windows and averaged the power spectra over epochs within lower or upper
240 quartile movement ranges, as well as quiescence (Figure 2E *top*). As expected, under
241 baseline conditions, the power spectra changed based on the magnitude of movement,
242 with SWA suppressed during movement compared to quiescence, and in the highest
243 quartile of activity compared to the lowest. Importantly, the same analysis applied to
244 data recorded after administration of LPS did not show changes in the power spectra
245 with increases in movement (Figure 2E *bottom*). Instead, following LPS administration,
246 SWA was elevated even during movement, rendering power spectra during movement
247 similar to those recorded during quiescence.

248 The analysis of Figure 2E suggests an effect of LPS on SWA during active
249 wakefulness. However, to quantify this effect, we would want to compare SWA recorded
250 during periods with identical movement profiles. To achieve this, we applied propensity

score matching (Supplementary Figure 2) to compare SWA across comparable distributions of movement recorded during baseline and Peak LPS. LPS caused a steep increase in movement-matched SWA (Figure 3A), though there was no significant difference between LPS doses (Table 1G). SWA during quiescent periods was increased by LPS treatment (Figure 3B), though this effect was mainly driven by aged animals (discussed later) and no direct comparisons showed differences between the adult LPS-only groups (Table 1H).

Cortical connectivity is unchanged in LPS after correcting for changes in activity

Under baseline conditions, we observed that alpha-band wPLI was positively correlated with movement (Supplementary Figure 6B; $r^{2=}0.435$, $p<0.05$), suggesting that the decrease in wPLI observed in LPS could be due to the reduction in movement following injection of LPS. This is indeed what was observed when we applied propensity score matching to the relationship between wPLI and movement. To obtain accurate measures of wPLI, we expanded the time window for movement analysis to 20 seconds, slightly reducing the temporal resolution of changes in activity level. The movement-matched alpha-band wPLI was unaffected by LPS (Figure 3C; Table 1I), indicating the absence of changes in wPLI after accounting for LPS-induced decreases in movement. wPLI during quiescence was also unaffected by LPS treatment (Figure 3D; Table 1J).

Neocortical cytokine levels correlate with changes in movement-matched SWA

We observed increases in cytokine levels following injection of LPS and systematic increases in SWA after accounting for the effect of LPS on movement. We next sought to determine if the magnitude of the increase in cytokine levels and the magnitude of the changes in brain activity were related for the measures that showed significant LPS effects. IL-6 levels correlated with increases in movement-matched SWA for LPS-only groups (Figure 4A; $r^{2=}0.662$, $p<0.00001$), as did MCP-1 levels (Figure 4B; $r^2=0.541$, $p=0.0014$).

Piroxicam attenuates the EEG slowing in LPS without affecting brain IL-6 levels or acute decreases in movement

Piroxicam is a non-selective cyclooxygenase inhibitor previously shown to attenuate acute behavioral changes induced by LPS[3, 23]. We first determined that 10mg/kg piroxicam administration prior to Low LPS did not affect neocortical levels of IL-6 or MCP-1 compared to Low LPS alone (Supplemental Figure 7A-B; Table 1A), indicating any effect of piroxicam electrophysiologically or behaviorally would be downstream of the initial pro-inflammatory cytokine response, similar to prior reports.

Piroxicam blunted the LPS-induced increase of overall SWA (i.e. before accounting for movement; Figure 5A *red*; Table 1C) and gamma power (Supplementary Figure 4B; Table 1D) but did not decrease the impact of LPS on wPLI (Figure 5B; Table 1E). Piroxicam did not alter movement during the peak hours following LPS injection compared to Low LPS-only animals (Figure 5C). However, the difference in movement between baseline and the final recording hour (the fourth hour post-LPS, not included in

'Peak LPS') was significantly smaller in 'PXM+Low LPS' relative to Low LPS alone (likelihood ratio test: $\chi^2(1)=16.625$, $p<0.0001$), suggesting that piroxicam-treated animals may recover more quickly. Piroxicam attenuated the LPS-induced increase in movement-matched SWA (Figure 3A; Table 1G). As with Low LPS alone, piroxicam did not change SWA during quiescent periods (Figure 3B; Table 1H). Further, piroxicam animals showed smaller movement-matched SWA changes than would have been predicted from IL-6 (Figure 4A *red*; For PXM prediction residuals, one-sample t-test vs zero: t=-3.78, df=6, p=0.0092) or MCP-1 levels (Figure 4B *red*; for PXM prediction residuals, one-sample t-test vs zero: t=-3.54, df=6, p=0.012).

Given prior data showing that piroxicam blunts the prostaglandin response to LPS by inhibiting COX activity[3, 23], and that prostaglandin D_2 acts as a powerful somnogen via downstream effects on adenosine signaling[24, 25], we further investigated the role of this pathway in LPS-induced SWA by testing the effect of caffeine citrate.

Repeated injection of caffeine diminishes LPS-induced EEG changes

Caffeine promotes wakefulness through antagonism at the A_{2A} adenosine receptor[42, 43], which is a downstream mediator of the somnogenic prostaglandin D_2 that is known to affect cortical arousal[25, 44, 45]. When animals were administered LPS in combination with caffeine citrate, they showed lower overall SWA (Figure 5A *blue*), higher gamma power (Supplementary Figure 4B), increased alpha-band wPLI, and increased movement compared to animals administered LPS with saline (Figure 5B-C; Table 1C-F). Caffeine blunted the effects of LPS on the movement-matched SWA compared to animals treated with LPS plus saline (Figure 3A; Table 1G). Caffeine did

not alter SWA during quiescence compared to saline-treated animals (Figure 3B; Table 1H). The effect of caffeine citrate treatment plus LPS on movement-matched wPLI relative to animals treated with saline plus LPS (Figure 3C) was strikingly similar to the effect of Vehicle versus Low LPS reported above (compare Figure 3C), though here the difference between the two was statistically significant (Table 1I). Caffeine pretreatment did not alter wPLI during quiescence relative to saline (Figure 3D; Table 1J).

Aged animals exhibit exaggerated EEG slowing during quiescence

As delirium is most relevant in aged populations[46], we repeated LPS experiments in aged mice and compared results to adult animals. As expected[47], aged mice compared to adults showed higher neocortical IL-6 as well as higher MCP-1 protein levels in response to LPS treatment (Supplementary Figure 6A-B; Table 1A-B). Aged animals demonstrated an increased overall SWA response to LPS compared to adult animals (Figure 5A *green*; Table 1C), though this was not observed for gamma power (Supplementary Figure 4B; Table 1D). Decreases in wPLI were exaggerated in aged animals (Figure 5B; Table 1E). LPS-driven decreases in movement were not different between aged animals and adults (Figure 5C; Table 1F). Increases in movement-matched SWA due to LPS were not different from adult animals (Figure 3A; Table 1G). Instead, SWA during quiescence was greatly increased in aged compared to adult animals (Figure 3B; Table1H), and this was the only significant contrast in the model. As stated above, changes in both movement-matched and quiescent alpha wPLI following LPS treatment were not significant in models including aged animals (Figure 3C-D; Table 1I-J).

Discussion

Inflammation-induced changes in cortical activity

Inflammation causes acute changes in brain activity and connectivity in hippocampus, where changes in synaptic plasticity may underlie cognitive deficits observed during delirium[48, 49]. Less is known about the effects of inflammation on neocortical activity. Our results show some alignment with previous findings in rodents[22, 50], where a much higher dose of LPS (1mg/kg) slowed hippocampal theta rhythms independently of changes in locomotion, though comparable effects were not observed in prefrontal cortex, suggesting the slowing is region-selective. The data presented here suggest a similar regional heterogeneity, as posterior increases in SWA were larger than anterior in High LPS animals, but this observation requires confirmation with further experiments. Posterior cortical SWA appears particularly important in delirium[14]. Previous studies have also described EEG slowing and decreases in alpha antero-posterior wPLI[50], but did not account for effects on movement[40] and also used a much higher dose of LPS (1mg/kg), making their results more likely to reflect somnolence rather than wakeful EEG activity[39].

Our findings with aged animals indicate an exaggerated biochemical and electrophysiological response to inflammation, but since the differences between aged and adult animals were only observed in quiescence, those electrophysiological effects could be secondary to increased hypoactivity. Further work is needed to determine whether this rise in SWA in mice during quiescence reflects hypoactive wakefulness or sleep, but the data suggest that inflammation in aged animals induces a hypoactive phenotype that is particularly prevalent in elderly patients[46].

364

365 **Inflammation-induced changes in cortical connectivity**

366 The finding that alpha-band wPLI connectivity changes were attributable to
367 changes in movement is potentially of clinical significance. The association of impaired
368 alpha-band wPLI with delirium stems from work in postoperative patients where delirium
369 is predominantly hypoactive[14, 29, 30]. In contrast, a study of delirium on emergence from
370 anesthesia in young children, which is typically hyperactive, found increased alpha band
371 connectivity during delirium[51]. In this context, reduced alpha-band wPLI may represent a
372 specific marker of hypoactive delirium and this possibility should be tested in a cohort of
373 patients including hypoactive and hyperactive delirium.

374

375 **Cytokine cascades contributing to inflammation**

376 We acknowledge important differences in approaches to the study of
377 inflammation in the mouse and human models. Notably we induced systemic
378 inflammation in the mouse model using LPS, but focused on brain inflammation as a
379 surrogate of neuroinflammatory hypotheses of delirium. In our recent work on delirium[14]
380 we studied plasma cytokines, a more distant surrogate of neuroinflammation. In the
381 current study, we specified *a priori* that IL-6 would be the primary cytokine of interest
382 due to its sensitivity to LPS[32], long half-life[33], and prior data from cerebrospinal fluid
383 studies of delirium[52]. We complemented this with study of MCP-1 based on our recent
384 paper[14]. Given redundancy in cytokine cascades, the next step is to understand local
385 neuronal, immune, and circuit dynamics of these inflammatory stimuli. We suggest that
386 inflammation drives EEG changes through induced release of prostaglandin D_2 and

subsequent effects on adenosine signaling, most likely in sleep and arousal centers in the hypothalamus and basal forebrain (Figure 6)[25]. Verification of the locus of adenosine's actions, and investigation of possible direct actions of adenosine on cortical circuits, awaits further experiments. As non-steroidal anti-inflammatory drugs should be avoided in vulnerable elderly patients, future studies should focus on the therapeutic benefit of targeted manipulation of adenosine signaling in this mouse model and in a clinical setting.

Translational relevance

Our focus has been on objective translational features of delirium that can be feasibly studied in the rodent. In contrast to studies of sepsis, where LPS is viewed as a suboptimal model[53], LPS is commonly used in rodent studies of the mechanisms of delirium because it produces a profound and consistent proinflammatory response[3, 22, 49]. Our approach was to model how this inflammatory response affects EEG activity during movement to avoid the confound of sleep. As elevated SWA during wakefulness is a key criterion for delirium and is often associated with inattention, another key criterion, our model has a plausible association with delirium. The cognitive features that define delirium include impaired attention, arousal, executive function, orientation to the environment and memory as well as perceptual disturbances. Because inflammatory agents such as LPS affect motivation and motor function in animal models, investigating the cognitive correlates of inflammation behaviorally in mice is complicated[39]. Instead, we present an animal model of inflammation-related SWA during wakefulness; establishing this animal model opens opportunities for testing hypotheses about

mechanisms and treatments for delirium and other inflammatory brain disorders. We consider this work to be complementary to work done with cognitive testing[3, 54], which itself has limitations regarding the characterization of a complex human disorder in mice. Importantly, we recently showed that inflammation-driven SWA correlates with delirium severity in humans[14], hence the ability to model this effect in mice and study mechanisms represents a major methodological advance. Furthermore, delirium, cognitive decline, and dementia are profound cognitive disorders associated with inflammation[2, 4, 5] as well as changes in SWA[13, 55, 56]. Hence understanding the mechanisms whereby inflammation drives SWA may illuminate the key pathophysiological mechanisms of cognitive impairment in a variety of disorders.

Future directions

The data presented here motivate future investigations into the mechanisms linking inflammation to changes in neural activity and connectivity. For example, previous studies have shown the acute behavioral effects of LPS are driven by peripheral IL-1B[49]; thus, it would be illuminating to measure plasma inflammatory markers in addition to measuring cortical cytokines. Future experiments should also identify specific receptor subtypes and other aspects of the signaling pathways involved in the link between neuroinflammation and changes in brain activity. For example, we tested caffeine, which is a non-specific adenosine receptor antagonist and has potential clinical application. Elucidating the roles of adenosine A_1 versus A_2 receptors would allow for more targeted drug development. In addition, future studies should include the effects of inflammation in mice modeling disorders associated with delirium, like

433 dementia. More broadly, the model presented here opens opportunities for testing the
434 roles of specific neuronal, glial, and immune cell types in the signaling cascade linking
435 inflammation to drastic changes in brain function[55, 56].

Authors' contributions

ZWS: Study design, data collection, data analysis, manuscript revision

ERJ: Study design, data collection, data analysis, writing first draft of paper

BMK: Study design, data analysis, manuscript revision

SMG: Data collection, data analysis, manuscript revision

CAM: Study design, manuscript revision

RDS: Study design, writing first draft of paper, manuscript revision

MIB: Study design, writing first draft of paper, manuscript revision

Acknowledgements

The authors thank Elizabeth A. Townsend, Payge A. Barnard, Jens Mellby, Hazel Bastien, and Matthieu Darracq for technical assistance.

Declaration of Interest

The authors declare no competing financial interests.

Funding

Supported by National Institutes of Health (R01 GM109086 to M. I. Banks; R01 AG063849 to R. D. Sanders), and the Department of Anesthesiology, School of Medicine and Public Health, University of Wisconsin, Madison, WI.

References

1. Sanders RD. Hypothesis for the pathophysiology of delirium: role of baseline brain network connectivity and changes in inhibitory tone. *Med Hypotheses* 2011; **77**: 140–3
2. Cunningham C, Maclullich AMJ. At the extreme end of the psychoneuroimmunological spectrum: delirium as a maladaptive sickness behaviour response. *Brain Behav Immun* 2013; **28**: 1–13
3. Griffin ÉW, Skelly DT, Murray CL, Cunningham C. Cyclooxygenase-1-Dependent Prostaglandins Mediate Susceptibility to Systemic Inflammation-Induced Acute Cognitive Dysfunction. *J Neurosci* 2013; **33**: 15248–58
4. Ramanan VK, Risacher SL, Nho K, et al. GWAS of longitudinal amyloid accumulation on 18F-florbetapir PET in Alzheimer's disease implicates microglial activation gene IL1RAP. *Brain* 2015; **138**: 3076–88
5. Whittington RA, Planel E, Terrando N. Impaired Resolution of Inflammation in Alzheimer's Disease: A Review. *Front Immunol* 2017; **8**: 1464
6. Merluzzi AP, Carlsson CM, Johnson SC, et al. Neurodegeneration, synaptic dysfunction, and gliosis are phenotypic of Alzheimer dementia. *Neurology* 2018; **91**: e436–43
7. Writing Committee of the WHO Consultation on Clinical Aspects of Pandemic (H1N1) 2009 Influenza, Bautista E, Chotpitayasunondh T, et al. Clinical aspects of pandemic 2009 influenza A (H1N1) virus infection. *N Engl J Med* 2010; **362**: 1708–19
8. Ely EW, Gautam S, Margolin R, et al. The impact of delirium in the intensive care unit on hospital length of stay. *Intensive Care Med* 2001; **27**: 1892–900
9. Pandharipande PP, Pun BT, Herr DL, et al. Effect of sedation with dexmedetomidine vs lorazepam on acute brain dysfunction in mechanically ventilated patients: the MENDS randomized controlled trial. *JAMA* 2007; **298**: 2644–53
10. Riker RR, Shehabi Y, Bokesch PM, et al. Dexmedetomidine vs midazolam for sedation of critically ill patients: a randomized trial. *JAMA* 2009; **301**: 489–99
11. Pandharipande PP, Girard TD, Jackson JC, et al. Long-term cognitive impairment after critical illness. *N Engl J Med* 2013; **369**: 1306–16
12. Rudolph JL, Jones RN, Levkoff SE, et al. Derivation and validation of a preoperative prediction rule for delirium after cardiac surgery. *Circulation* 2009; **119**: 229–36
13. Ponten SC, Tewarie P, Slooter AJC, Stam CJ, van Dellen E. Neural network modeling of EEG patterns in encephalopathy. *J Clin Neurophysiol* 2013; **30**: 545–52
14. Tanabe S, Mohanty R, Lindroth H, et al. Cohort study into the neural correlates of postoperative delirium: the role of connectivity and slow-wave activity. *Br J Anaesth* 2020; **125**: 55–66
15. Nir Y, Andrillon T, Marmelshtein A, et al. Selective neuronal lapses precede human cognitive lapses following sleep deprivation. *Nat Med* 2017; **23**: 1474–80
16. Casey CP, Lindroth H, Mohanty R, et al. Postoperative delirium is associated with increased plasma neurofilament light. *Brain* 2020; **143**: 47–54
17. Yasuda T, Yoshida H, Garcia-Garcia F, Kay D, Krueger JM. Interleukin-1beta has a role in cerebral cortical state-dependent electroencephalographic slow-wave activity. *Sleep* 2005; **28**: 177–84

18. Taishi P, Churchill L, Wang M, et al. TNFalpha siRNA reduces brain TNF and EEG delta wave activity in rats. *Brain Res* 2007; **1156**: 125–32
19. Krueger JM, Clinton JM, Winters BD, et al. Involvement of cytokines in slow wave sleep. *Prog Brain Res* 2011; **193**: 39–47
20. Plaschke K, Fichtenkamm P, Schramm C, et al. Early postoperative delirium after open-heart cardiac surgery is associated with decreased bispectral EEG and increased cortisol and interleukin-6. *Intensive Care Med* 2010; **36**: 2081–9
21. Trzepacz PT, Leavitt M, Ciongoli K. An animal model for delirium. *Psychosomatics* 1992; **33**: 404–15
22. Mamad O, Islam MN, Cunningham C, Tsanov M. Differential response of hippocampal and prefrontal oscillations to systemic LPS application. *Brain Res* 2018; **1681**: 64–74
23. Teeling JL, Cunningham C, Newman TA, Perry VH. The effect of non-steroidal anti-inflammatory agents on behavioural changes and cytokine production following systemic inflammation: Implications for a role of COX-1. *Brain Behav Immun* 2010; **24**: 409–19
24. Qu W-M, Huang Z-L, Xu X-H, et al. Lipocalin-type prostaglandin D synthase produces prostaglandin D2 involved in regulation of physiological sleep. *Proc Natl Acad Sci U S A* 2006; **103**: 17949–54
25. Saper CB, Romanovsky AA, Scammell TE. Neural circuitry engaged by prostaglandins during the sickness syndrome. *Nat Neurosci* 2012; **15**: 1088–95
26. Hartmann M, Czok G. [Pharmacokinetics of caffeine in mice and its modification by ethanol]. *Z Ernahrungswiss* 1980; **19**: 215–27
27. Banks MI, Krause BM, Endemann CM, et al. Cortical functional connectivity indexes arousal state during sleep and anesthesia. *NeuroImage* 2020; **211**: 116627
28. Vinck M, Oostenveld R, van Wingerden M, Battaglia F, Pennartz CMA. An improved index of phase-synchronization for electrophysiological data in the presence of volume-conduction, noise and sample-size bias. *NeuroImage* 2011; **55**: 1548–65
29. van Dellen E, van der Kooi AW, Numan T, et al. Decreased functional connectivity and disturbed directionality of information flow in the electroencephalography of intensive care unit patients with delirium after cardiac surgery. *Anesthesiology* 2014; **121**: 328–35
30. Numan T, Slooter AJC, van der Kooi AW, et al. Functional connectivity and network analysis during hypoactive delirium and recovery from anesthesia. *Clin Neurophysiol* 2017; **128**: 914–24
31. Ho DE, Imai K, King G, Stuart EA. Matching as Nonparametric Preprocessing for Reducing Model Dependence in Parametric Causal Inference. *Polit Anal* 2007; **15**: 199–236
32. Skelly DT, Hennessy E, Dansereau M-A, Cunningham C. A systematic analysis of the peripheral and CNS effects of systemic LPS, IL-1β, [corrected] TNF-α and IL-6 challenges in C57BL/6 mice. *PloS One* 2013; **8**: e69123
33. Oda S, Hirasawa H, Shiga H, Nakanishi K, Matsuda K, Nakamua M. Sequential measurement of IL-6 blood levels in patients with systemic inflammatory response syndrome (SIRS)/sepsis. *Cytokine* 2005; **29**: 169–75

546 34. Munster BCV, Korevaar JC, Zwinderman AH, Levi M, Wiersinga WJ, Rooij SED.
547 Time-Course of Cytokines During Delirium in Elderly Patients with Hip Fractures. *J Am*
548 *Geriatr Soc* 2008; **56**: 1704–9
549 35. Bates D, Mächler M, Bolker B, Walker S. Fitting Linear Mixed-Effects Models
550 Using lme4. *J Stat Softw* 2015; **67**: 1–48
551 36. Lenth R, Buerkner P, Herve M, Love J, Riebl H, Singmann H. emmeans:
552 Estimated Marginal Means, aka Least-Squares Means [Internet]. 2020 [cited 2020 Aug
553 19]. Available from: https://CRAN.R-project.org/package=emmeans
554 37. Labrenz F, Wrede K, Forsting M, et al. Alterations in functional connectivity of
555 resting state networks during experimental endotoxemia - An exploratory study in
556 healthy men. *Brain Behav Immun* 2016; **54**: 17–26
557 38. Dantzer R, O'Connor JC, Freund GG, Johnson RW, Kelley KW. From
558 inflammation to sickness and depression: when the immune system subjugates the
559 brain. *Nat Rev Neurosci* 2008; **9**: 46–56
560 39. Cunningham C, Sanderson DJ. Malaise in the water maze: untangling the effects
561 of LPS and IL-1β on learning and memory. *Brain Behav Immun* 2008; **22**: 1117–27
562 40. Hansen IH, Agerskov C, Arvastson L, Bastlund JF, Sørensen HBD, Herrik KF.
563 Pharmaco-electroencephalographic responses in the rat differ between active and
564 inactive locomotor states. *Eur J Neurosci* 2019; **50**: 1948–71
565 41. Maloney KJ, Cape EG, Gotman J, Jones BE. High-frequency gamma
566 electroencephalogram activity in association with sleep-wake states and spontaneous
567 behaviors in the rat. *Neuroscience* 1997; **76**: 541–55
568 42. Huang Z-L, Qu W-M, Eguchi N, et al. Adenosine A 2A , but not A 1 , receptors
569 mediate the arousal effect of caffeine. *Nat Neurosci* Nature Publishing Group; 2005; **8**:
570 858–9
571 43. Yacoubi ME, Ledent C, Ménard J-F, Parmentier M, Costentin J, Vaugeois J-M.
572 The stimulant effects of caffeine on locomotor behaviour in mice are mediated through
573 its blockade of adenosine A2A receptors. *Br J Pharmacol* 2000; **129**: 1465–73
574 44. Terao A, Matsumura H, Saito M. Interleukin-1 Induces Slow-Wave Sleep at the
575 Prostaglandin D2-Sensitive Sleep-Promoting Zone in the Rat Brain. *J Neurosci* Society
576 for Neuroscience; 1998; **18**: 6599–607
577 45. Scammell T, Gerashchenko D, Urade Y, Onoe H, Saper C, Hayaishi O.
578 Activation of ventrolateral preoptic neurons by the somnogen prostaglandin D2. *Proc*
579 *Natl Acad Sci* National Academy of Sciences; 1998; **95**: 7754–9
580 46. Fong TG, Tulebaev SR, Inouye SK. Delirium in elderly adults: diagnosis,
581 prevention and treatment. *Nat Rev Neurol* 2009; **5**: 210–20
582 47. Murtaj V, Belloli S, Di Grigoli G, et al. Age and Sex Influence the Neuro-
583 inflammatory Response to a Peripheral Acute LPS Challenge. *Front Aging Neurosci*
584 2019; **11**: 299
585 48. Wang D-S, Zurek AA, Lecker I, et al. Memory deficits induced by inflammation
586 are regulated by α5-subunit-containing GABAA receptors. *Cell Rep* 2012; **2**: 488–96
587 49. Skelly DT, Griffin ÉW, Murray CL, et al. Acute transient cognitive dysfunction and
588 acute brain injury induced by systemic inflammation occur by dissociable IL-1-
589 dependent mechanisms. *Mol Psychiatry* 2019; **24**: 1533–48

50. Albrecht MA, Vaughn CN, Erickson MA, Clark SM, Tonelli LH. Time and frequency dependent changes in resting state EEG functional connectivity following lipopolysaccharide challenge in rats. *PLOS ONE* 2018; **13**: e0206985
51. Martin JC, Liley DTJ, Harvey AS, Kuhlmann L, Sleigh JW, Davidson AJ. Alterations in the functional connectivity of frontal lobe networks preceding emergence delirium in children. *Anesthesiology* 2014; **121**: 740–52
52. Cape E, Hall RJ, van Munster BC, et al. Cerebrospinal fluid markers of neuroinflammation in delirium: A role for interleukin-1β in delirium after hip fracture. *J Psychosom Res* 2014; **77**: 219–25
53. Lewis AJ, Seymour CW, Rosengart MR. Current Murine Models of Sepsis. *Surg Infect* 2016; **17**: 385–93
54. Davis DHJ, Skelly DT, Murray C, et al. Worsening cognitive impairment and neurodegenerative pathology progressively increase risk for delirium. *Am J Geriatr Psychiatry Off J Am Assoc Geriatr Psychiatry* 2015; **23**: 403–15
55. Babiloni C, De Pandis MF, Vecchio F, et al. Cortical sources of resting state electroencephalographic rhythms in Parkinson's disease related dementia and Alzheimer's disease. *Clin Neurophysiol* 2011; **122**: 2355–64
56. Nakamura A, Cuesta P, Fernández A, et al. Electromagnetic signatures of the preclinical and prodromal stages of Alzheimer's disease. *Brain J Neurol* 2018; **141**: 1470–85

Tables

Measure	Likelihood Ratio Test / Pairwise Comparison	n_1,n_2	p-value	Measure	Likelihood Ratio Test / Pairwise Comparison	n_1,n_2	p-value
A **IL-6**	$\chi^2(4) = 29.0$		<0.0001	**B** **MCP-1**	$\chi^2(4) = 29.1$		<0.0001
	VEH vs Low LPS	5,18	0.68		VEH vs Low LPS	5,18	0.87
	VEH vs High LPS	5,8	0.0004		VEH vs High LPS	5,8	0.0003
	Low LPS vs High LPS	18,8	0.0002		Low LPS vs High LPS	18,8	<0.0001
	VEH vs PXM+Low LPS	5,12	0.23		VEH vs PXM+Low LPS	5,12	0.12
	Low LPS vs PXM+Low LPS	18,12	0.69		Low LPS vs PXM+Low LPS	18,12	0.17
	Low LPS vs Aged Low LPS	18,13	0.0033		Low LPS vs Aged Low LPS	18,13	0.014
C **SWA**	$\chi^2(4) = 87.8$		<0.0001	**D** **gamma**	$\chi^2(4) = 78.6$		<0.0001
	VEH vs Low LPS	7,17	<0.0001		VEH vs Low LPS	7,17	<0.0001
	VEH vs High LPS	7,8	<0.0001		VEH vs High LPS	7,8	<0.0001
	Low LPS vs High LPS	17,8	0.041		Low LPS vs High LPS	17,8	0.043
	VEH vs PXM+Low LPS	7,8	0.72		VEH vs PXM+Low LPS	7,8	0.5
	Low LPS vs PXM+Low LPS	17,8	<0.0001		Low LPS vs PXM+Low LPS	17,8	<0.0001
	Low LPS vs Aged Low LPS	17,14	0.025		Low LPS vs Aged Low LPS	17,14	0.36
Caffeine	$\chi^2(1) = 36.6$	8,10	<0.001	Caffeine	$\chi^2(1) = 61.5$	8,10	<0.0001
E **wPLI**	$\chi^2(4) = 26.2$		<0.0001	**F** **Movt**	$\chi^2(4) = 18.8$		0.00085
	VEH vs Low LPS	7,17	0.011		VEH vs Low LPS	7,17	0.014
	VEH vs High LPS	7,8	0.002		VEH vs High LPS	7,8	0.0005
	Low LPS vs High LPS	17,8	0.61		Low LPS vs High LPS	17,8	0.25
	VEH vs PXM+Low LPS	7,8	0.063		VEH vs PXM+Low LPS	7,8	0.23
	Low LPS vs PXM+Low LPS	17,8	1		Low LPS vs PXM+Low LPS	17,8	0.83
	Low LPS vs Aged Low LPS	17,12	0.031		Low LPS vs Aged Low LPS	17,14	0.99
Caffeine	$\chi^2(1) = 18.2$	8,10	0.0002	Caffeine	$\chi^2(1) = 18.8$	8,10	<0.0001
G **SWA** $_{\text{Movt-matched}}$	$\chi^2(4) = 21.5$		0.00025	**H** **SWA** $_{\text{Quiescent}}$	$\chi^2(4) = 19.7$		0.00057
	VEH vs Low LPS	7,16	0.0086		VEH vs Low LPS	6,16	0.67
	VEH vs High LPS	7,5	0.0057		VEH vs High LPS	6,5	0.32
	Low LPS vs High LPS	16,5	0.77		Low LPS vs High LPS	16,5	0.82
	VEH vs PXM+Low LPS	7,7	1		VEH vs PXM+Low LPS	6,7	1
	Low LPS vs PXM+Low LPS	16,7	0.013		Low LPS vs PXM+Low LPS	16,7	0.83
	Low LPS vs Aged Low LPS	16,13	0.99		Low LPS vs Aged Low LPS	16,13	0.0086
Caffeine	$\chi^2(1) = 3.98$	8,8	0.046	Caffeine	$\chi^2(1) = 2.61$	8,8	0.11
I **wPLI** $_{\text{Movt-matched}}$	$\chi^2(4) = 6.39$		0.17	**J** **wPLI** $_{\text{Quiescent}}$	$\chi^2(4) = 4.77$		0.31
Caffeine	$\chi^2(1) = 7.0$	8,6	0.0082	Caffeine	$\chi^2(1) = 1.49$	8,8	0.22

Table 1. Statistical modeling results. Shown are results of likelihood ratio tests for both the main models and models comparing caffeine experiments, along with associated sample counts (n_1, n_2), p-values and the results of pairwise comparisons. Effects of LPS were tested by comparing models with and without the group-by-epoch interaction (or group itself for cytokine data) using likelihood ratio tests. Caffeine

619 experiments were fit in separate models together with equivalent saline controls; since
620 there are only two factor levels no pairwise comparisons are needed. Post-hoc
621 comparisons used the Kenward-Roger method and p-values for pairwise comparisons
622 were adjusted for multiple comparisons by estimating a multivariate t-distribution using
623 the emmeans package for R[36].
624

Figure Captions

Figure 1. Proinflammatory cytokine levels in neocortex after LPS treatment. A. Shown are interleukin-6 (IL-6) protein concentrations measured via ELISA in neocortical homogenate samples from mice (including animals with and without EEG implant) euthanized four hours after LPS injection. Each point represents log IL-6 concentration (pg/ml) from samples obtained bilaterally from anterior (ant; *purple triangles*) or posterior cortex (post; *green circles*). Overlaid symbols (*black*) represent the within-group mean across all samples. Error bars represent ± SEM. * indicates significant difference from Vehicle. # indicates significant difference from Low LPS. **B.** Monocyte chemoattractant protein-1 (MCP-1) protein concentration values are shown. MCP-1 samples below the threshold of detection were set to the square root of the lowest observed quantity (1.13). LPS, lipopolysaccharide; VEH, vehicle.

Figure 2. Generalized slowing of EEG and disrupted functional connectivity following LPS injection. A. Representative time-domain EEG signals during the pre-injection baseline hour (*left*) and two hours post-injection (*right*) are shown for animals that received either a saline “Vehicle” (*top*) or 25 µg/kg “Low” LPS injection (*bottom*)**.** Traces were selected based on having mean SWA values approximately equal to the mean SWA over the entire hour. **B.** The time series of SWA (2-4Hz) normalized to mean spectral power (2-80Hz) are shown for the different LPS doses. Symbols represent the mean percent change in SWA from baseline across all animals at each LPS dose at each recording hour. Error bars represent ± SEM. **C.** Time series of alpha-band (13-20Hz) anterior-posterior weighted-phase lag index (wPLI), a measure of

functional connectivity. **D.** The time series of movement for each LPS dose is shown. Symbols represent the mean percent change in movement from baseline across all animals at each dose of LPS at each recording hour. Error bars represent ± SEM. **E.** Example EEG power spectra separated according to movement magnitude. Power spectra were calculated in overlapping 4-second windows and aligned with movement epochs, then data were binned into quiescence (i.e. zero movement, *left*), lower quartile movement (*middle*), or upper quartile movement (*right*), and averaged. Pre-injection spectra ("baseline"; *gray*) and average spectra of 1-3 hours post-injection ("peak"; *black*), averaged across four EEG channels, are shown from animals that received either Vehicle (*top*) or a 25 µg/kg "Low" dose of LPS (*bottom*). LPS, lipopolysaccharide; SWA, slow-wave activity; VEH, vehicle; wPLI, weighted phase lag index.

Figure 3. Changes in SWA and alpha-band wPLI during movement or quiescence. **A.** Movement-matched SWA values at baseline (*gray*) or peak LPS (*black*). Lines indicate mean log SWA values for individual animals while symbols represent group averages. Error bars indicate ± SEM. * indicates significant difference of differences from Vehicle. # indicates significant difference of differences from Low LPS. † indicates significant difference of differences from Saline + Low LPS. **B.** SWA during quiescence. **C.** Movement-matched alpha-band wPLI. **D.** Alpha wPLI during quiescence. CAFc, caffeine citrate; LPS, lipopolysaccharide; PXM, piroxicam; SWA, slow-wave activity; VEH, vehicle; wPLI, weighted phase lag index.

Figure 4. Cytokine correlations with changes in movement-matched SWA. A. Scatterplot of the change in movement matched SWA from baseline to peak LPS versus log IL-6 concentration. Markers represent values for individual animals. The line indicates the polynomial least-squares fit (using the MATLAB function "regress") for LPS-only groups, and the shading indicates the 95% prediction interval of the regression line. The R^2 value for the fit is also indicated. **B.** Scatterplot of the change in movement matched SWA from baseline to peak versus log MCP-1 concentration. IL-6, interleukin-6; LPS, lipopolysaccharide; MCP-1, Monocyte chemoattractant protein-1; PXM, piroxicam; SWA, slow-wave activity; VEH, vehicle.

Figure 5. EEG and movement time course summary across groups

A. The time series of SWA (2-4Hz) normalized to mean spectral power (2-80Hz) are shown for all LPS groups (Vehicle, Low LPS, and High LPS are the same as in Figure. 2). Symbols represent the mean percent change in SWA from baseline across all animals at each LPS dose at each recording hour. Error bars represent ± SEM. **B.** Gamma power time series. **C.** Alpha wPLI time series. **D.** Movement time series. Bars indicate ± SEM. CAFc, caffeine citrate; LPS, lipopolysaccharide; PXM, piroxicam; SWA, slow-wave activity; VEH, vehicle; wPLI, weighted phase lag index.

Figure 6. Working model of inflammation-driven SWA

Our working model of the generation of wakeful SWA relevant to delirium begins with systemic inflammation leading to Leptomeningeal-blood barrier inflammation, release of prostaglandin D_2 (PGD_2) and, via prostaglandin D receptor activation, release of

693 adenosine. The enrichment of prostaglandin D receptors on the basal forebrain and
694 hypothalamus suggests that adenosine then acts at the nearby arousal centres to
695 promote sleep, and cortical SWA during wake. However, prostaglandin D synthase is
696 diffusely expressed by the leptomeninges, and found in CSF, and so we cannot exclude
697 additional direct cortical actions to induce SWA. Understanding whether the SWA
698 reflects global or local slow waves seems a critical next step to determine whether
699 delirium involves activation of sleep centres (likely inducing global slow waves that
700 typically occur early in the night) or also local changes that support more restricted SWA
701 (that may reflect local changes in adenosine related to PGD_2 or metabolism).

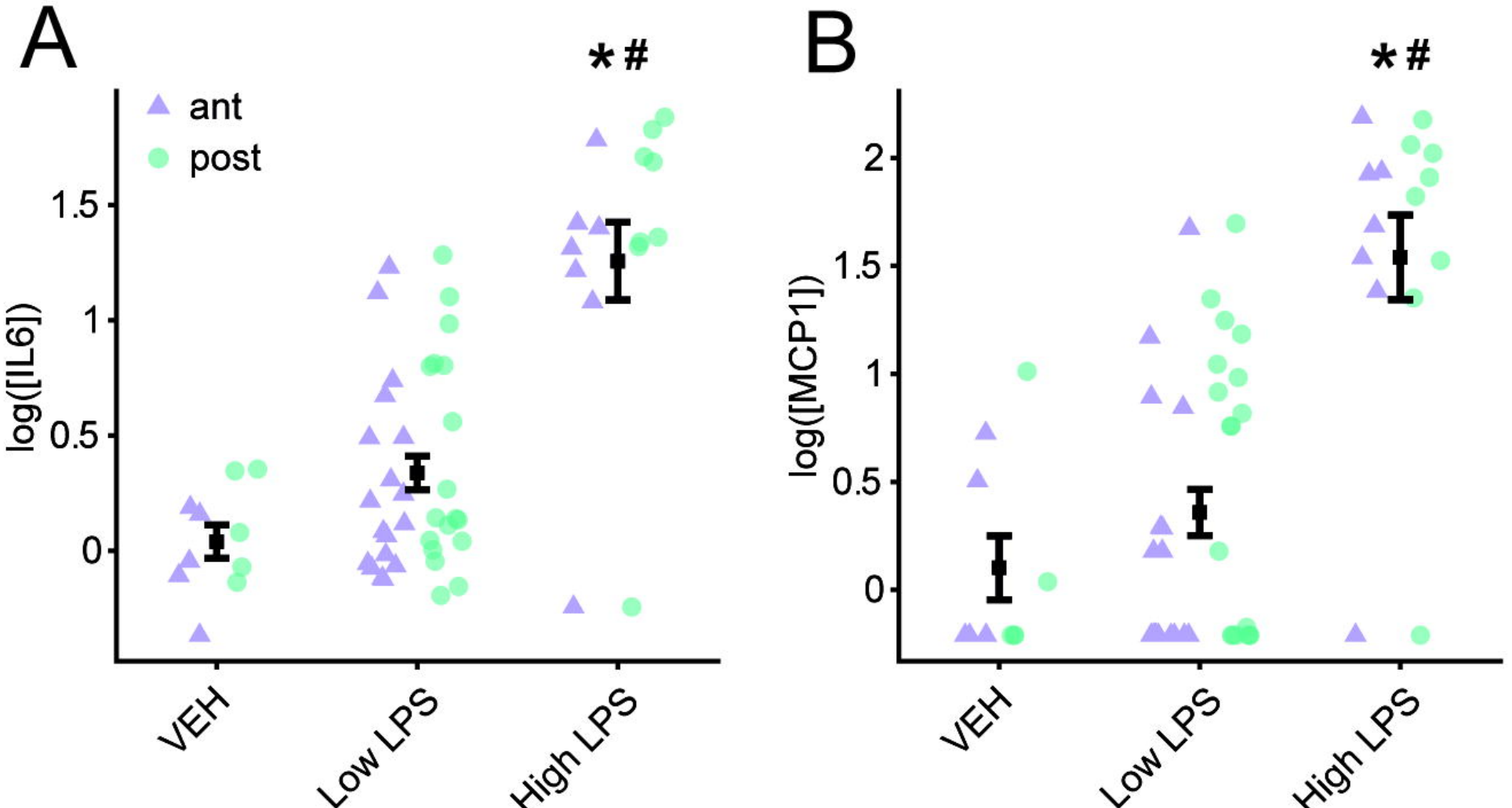
A
*#
ant
post
log([IL6])
1.5
1
0.5
0
VEH
Low LPS
High LPS
B
*#
log([MCP1])
2
1.5
1
0.5
0
VEH
Low LPS
High LPS

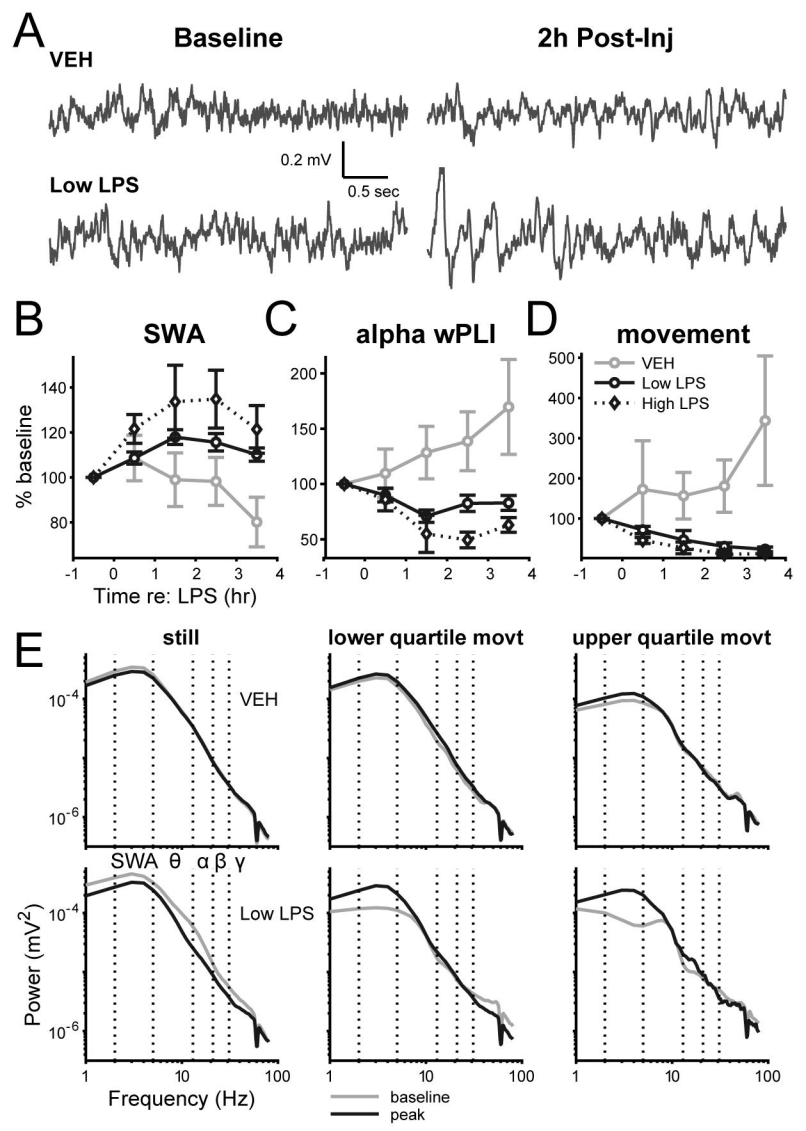
A
VEH
Baseline
2h Post-Inj
0.2 mV
0.5 sec
Low LPS
B
SWA
% baseline
Time re: LPS (hr)
C
alpha wPLI
D
movement
VEH
Low LPS
High LPS
E
still
lower quartile movt
upper quartile movt
VEH
SWA θ α β γ
Low LPS
Power (mV²)
Frequency (Hz)
baseline
peak

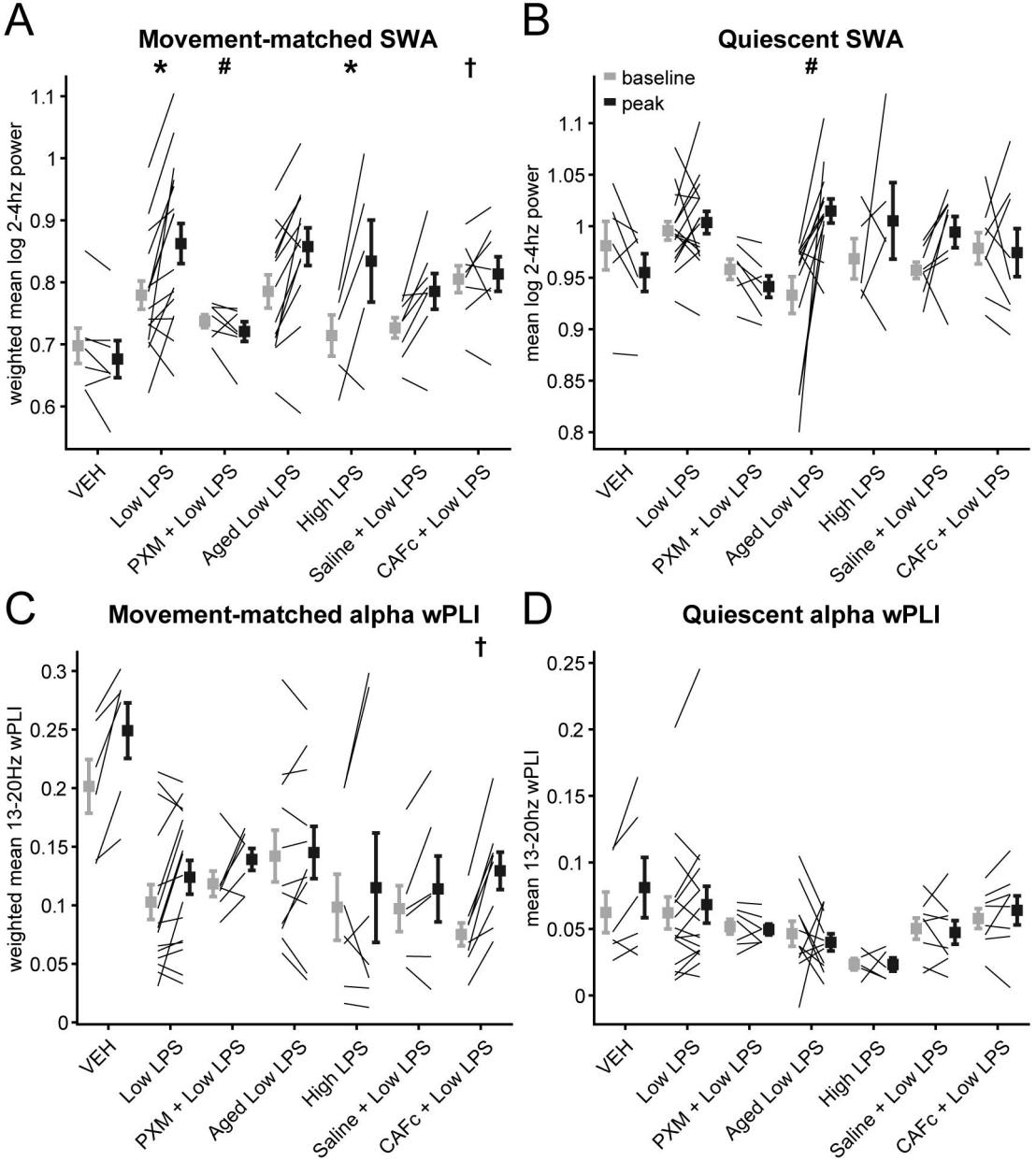
A
Movement-matched SWA
*
#
*
†
weighted mean log 2-4hz power
1.1
1
0.9
0.8
0.7
0.6
VEH
Low LPS
PXM + Low LPS
Aged Low LPS
High LPS
Saline + Low LPS
CAFc + Low LPS
B
Quiescent SWA
baseline
peak
#
mean log 2-4hz power
1.1
1.05
1
0.95
0.9
0.85
0.8
VEH
Low LPS
PXM + Low LPS
Aged Low LPS
High LPS
Saline + Low LPS
CAFc + Low LPS
C
Movement-matched alpha wPLI
†
weighted mean 13-20Hz wPLI
0.3
0.25
0.2
0.15
0.1
0.05
0
VEH
Low LPS
PXM + Low LPS
Aged Low LPS
High LPS
Saline + Low LPS
CAFc + Low LPS
D
Quiescent alpha wPLI
mean 13-20hz wPLI
0.25
0.2
0.15
0.1
0.05
0
VEH
Low LPS
PXM + Low LPS
Aged Low LPS
High LPS
Saline + Low LPS
CAFc + Low LPS

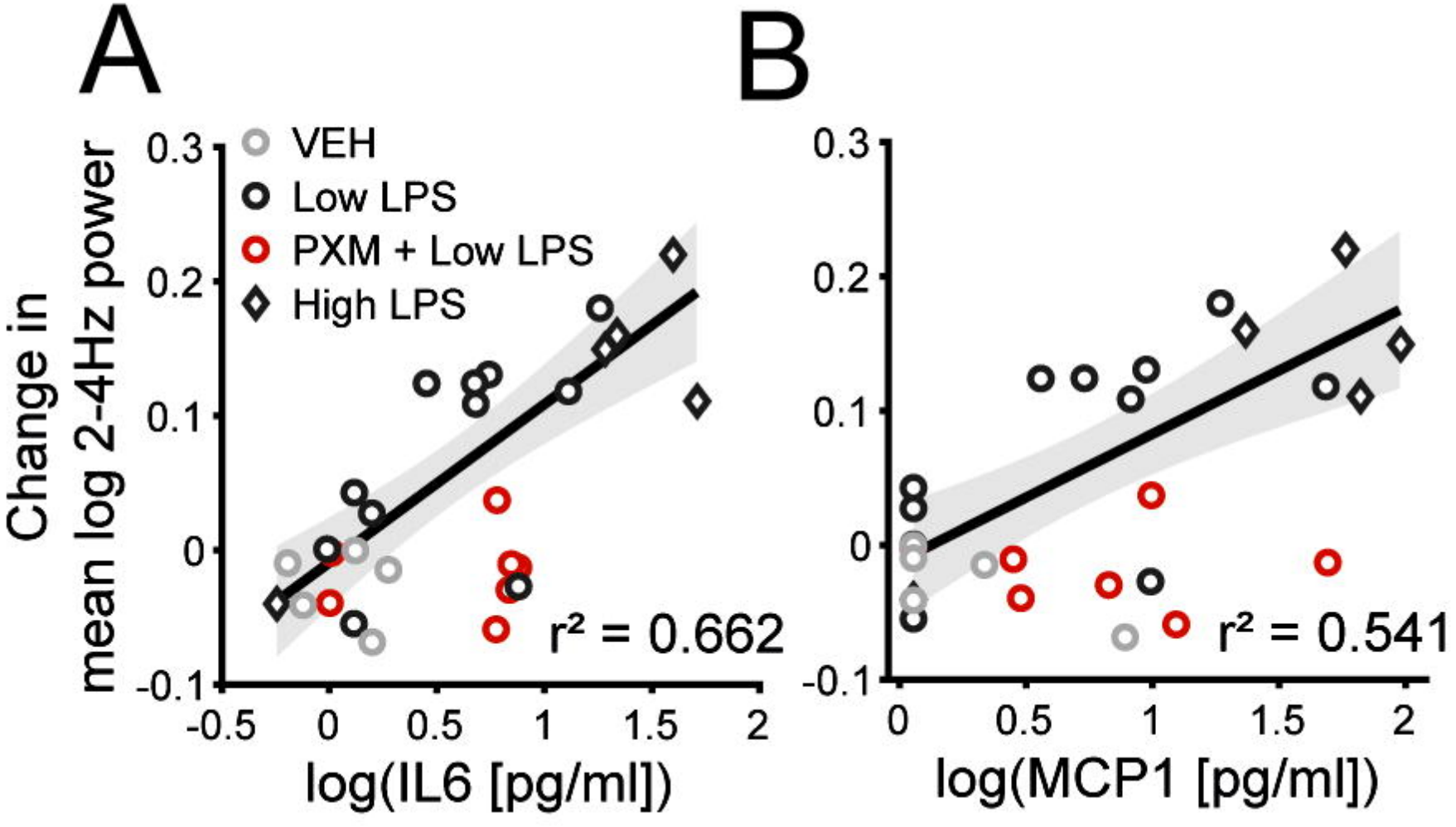
A
B
VEH
Low LPS
PXM + Low LPS
High LPS
Change in mean log 2-4Hz power
0.3
0.2
0.1
0
-0.1
-0.5
0
0.5
1
1.5
2
log(IL6 [pg/ml])
r² = 0.662
log(MCP1 [pg/ml])
r² = 0.541

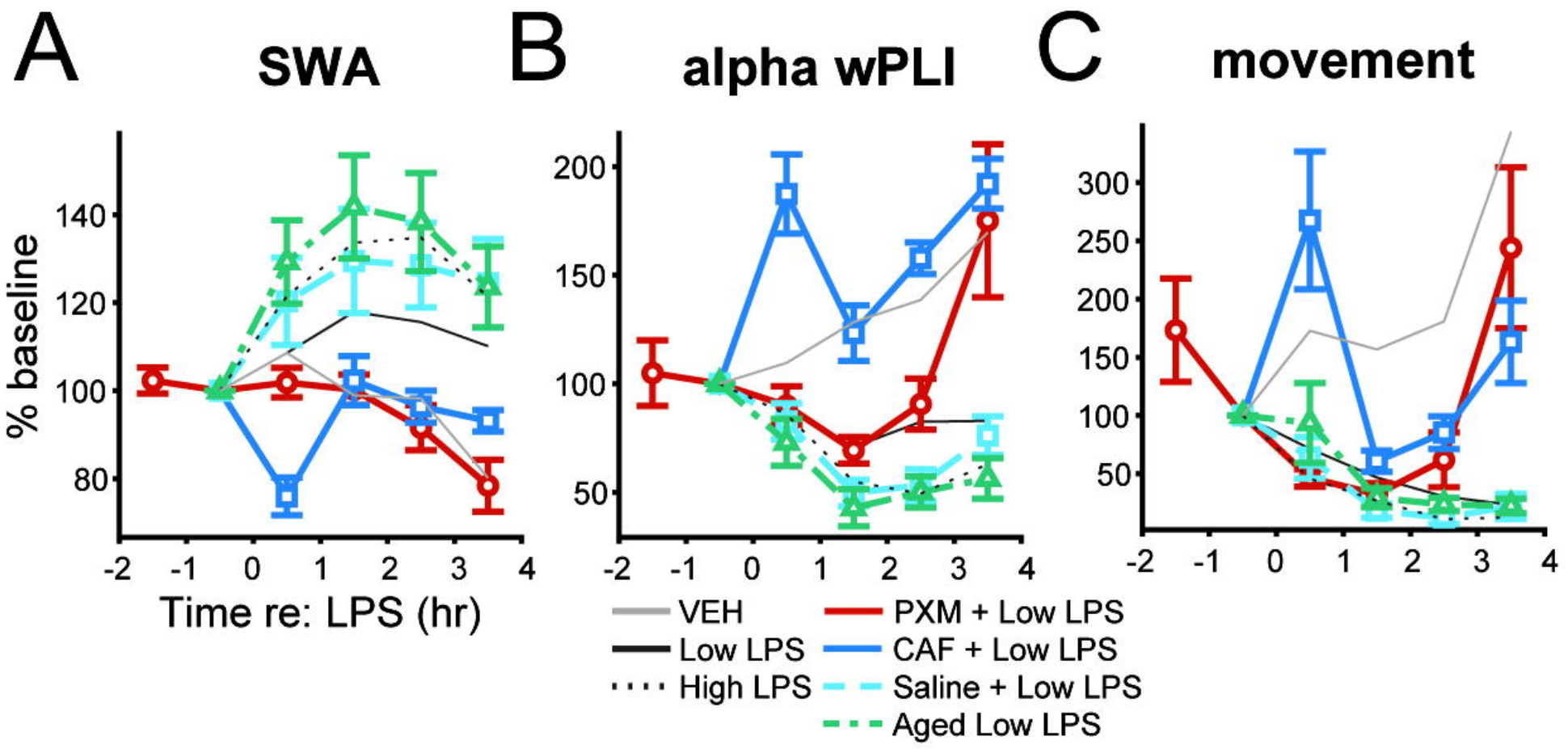
A
SWA
B
alpha wPLI
C
movement
% baseline
140
120
100
80
200
150
100
50
300
250
200
150
100
50
-2
-1
0
1
2
3
4
Time re: LPS (hr)
VEH
Low LPS
High LPS
PXM + Low LPS
CAF + Low LPS
Saline + Low LPS
Aged Low LPS

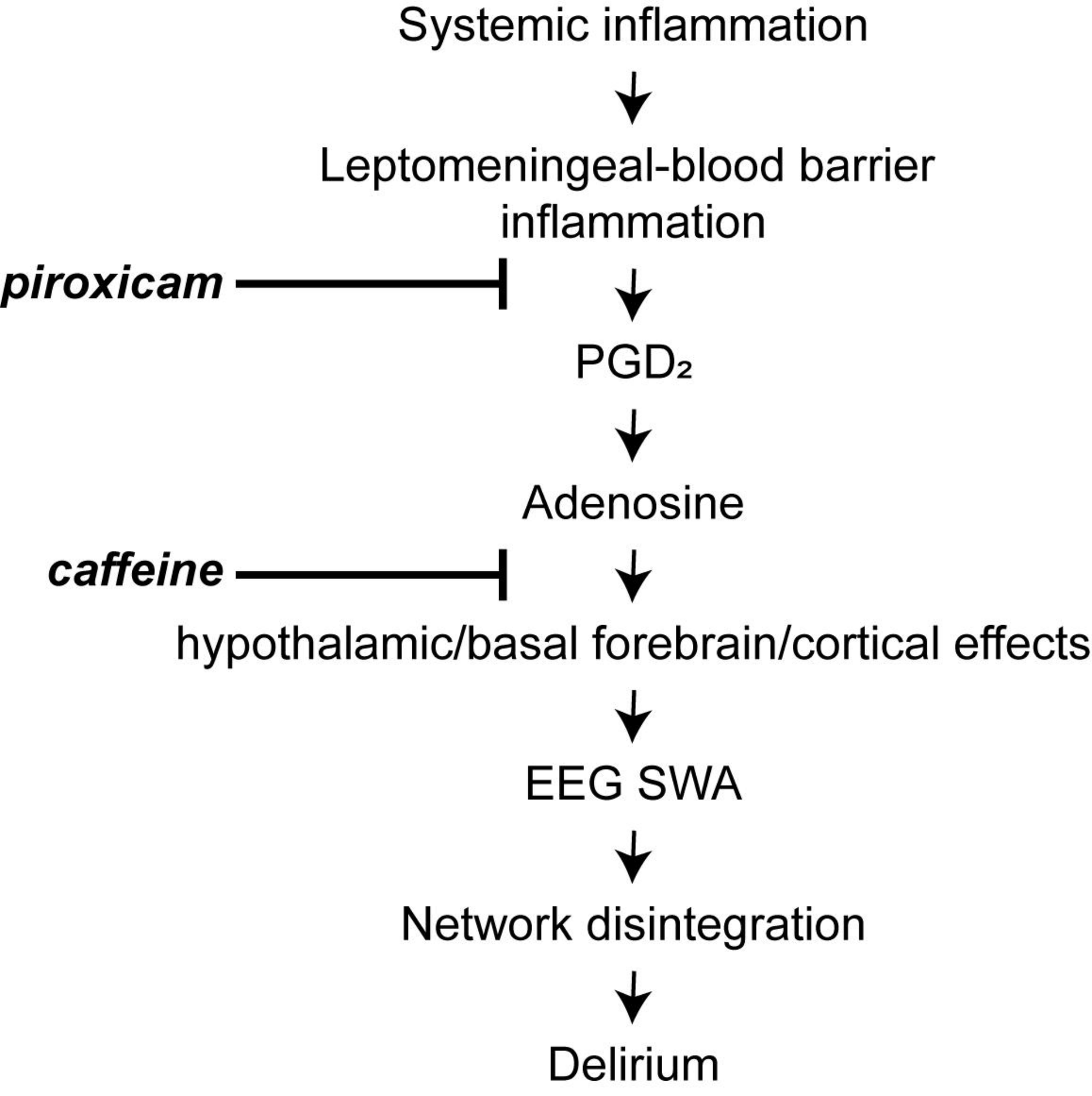
Systemic inflammation
Leptomeningeal-blood barrier inflammation
piroxicam
PGD2
Adenosine
caffeine
hypothalamic/basal forebrain/cortical effects
EEG SWA
Network disintegration
Delirium